VIP **Platinum Nanocatalyst**

A Highly Durable Platinum Nanocatalyst for Proton Exchange Membrane Fuel Cells: Multiarmed Starlike Nanowire Single Crystal**

Shuhui Sun, Gaixia Zhang, Dongsheng Geng, Yougui Chen, Ruying Li, Mei Cai, and Xueliang Sun*

Despite significant recent advances, the long-term durability of Pt catalyst at the cathode is still being recognized as one of the key challenges that must be addressed before the commercialization of proton exchange membrane fuel cells (PEMFCs).[1,2] The loss of Pt electrochemical surface area (ECSA) over time, because of corrosion of the carbon support and Pt dissolution/aggregation/Oswald ripening, is considered one of the major contributors to the degradation of fuel cell performance.[3] Up to now, highly dispersed Pt nanoparticles (NPs, 2–5 nm) on carbon supports are still being widely used as the state-of-the-art commercial catalysts, and most reported studies are focused on nanoparticles of Pt.[4] However, Pt with nanosized particle morphologies has high surface energies, thereby inducing severe Oswald ripening and/or grain growth during fuel cell operation.

One-dimensional (1D) nanostructures of Pt, such as nanowires (NWs) and nanotubes (NTs), have been demonstrated to overcome the drawbacks of NPs in fuel cells, owning to their unique 1D morphologies.[5–11] Yan et al.[11] reported that unsupported Pt nanotubes exhibit much enhanced catalytic activity and durability as fuel cell cathode catalyst. Sun et al.[9] and Zhou et al.[10] reported the improved oxygen reduction reaction (ORR) activities of Pt NWs at the cathode under fuel cell operating conditions. However, up to now, the durability of Pt NW-based electrocatalysts has never been reported in the literature.

Here we describe a new approach to address, for the first time, both the activity and durability issues by using carbon-supported multiarmed starlike Pt nanowires (starlike PtNW/C) as electrocatalysts. Interestingly, the durability can be further improved by eliminating the carbon support, that is, using unsupported Pt nanowires as the cathode catalyst. As a result of their unique 1D morphology, the starlike Pt nanowire electrocatalyst can provide various advantages. First, the

[*] Dr. S. Sun,[+] Dr. G. Zhang,[+] Dr. D. Geng, Y. Chen, R. Li, Prof. X. Sun
Department of Mechanical and Materials Engineering
The University of Western Ontario
London, Ontario N6A 5B9 (Canada)
Fax: (+1) 519-661-3020
E-mail: xsun@eng.uwo.ca

Dr. M. Cai
General Motors R&D Center, Warren, MI 48090-9055 (USA)

[+] These authors contributed equally to this work.

interconnected network consists of multiarmed, star-shaped 1D NWs with arm lengths of tens of nanometers which makes the Pt less vulnerable to dissolution, Ostwald ripening, and aggregation during fuel cell operation compared to Pt nanoparticles.[11] Second, this network structure reduces the number of embedded electrocatalyst sites in the micropores of the carbon supports relative to those in nanogrannular Pt. Third, the mass transfer within the electrode can be effectively facilitated by networking the anisotropic morphology.[12]

Carbon-supported multiarmed starlike platinum nanowires were synthesized by the chemical reduction of a Pt precursor with formic acid in aqueous solution at room temperature and under ambient atmosphere.[13] No surfactant, which is usually harmful for catalytic activities, was used in the experiments.

Figure 1 A and B show the representative scanning electron microscopy (SEM) and transmission electron microscopy (TEM) images, respectively, of carbon-supported Pt nanowires at 40 wt % loading of Pt. It can be seen that the as-synthesized Pt is nanostar-shaped, being composed of several short arms of Pt nanowires. The number of arms of each nanostar is found to vary ranging from several to over ten. Occasionally, single-armed nanowires standing on the carbon surface can also be observed. Diameter and length of the arms of starlike Pt nanowires are about 4 nm and 15 nm, respectively. More interestingly, from the connected atomic arrangement shown in the high-resolution TEM (HRTEM) images (see Figure S1 in the Supporting Information and the inset in Figure 1 B), the nanostar is found to be a single crystal. The fast Fourier transform (FFT; see inset in Figure S1) of the original HRTEM image shows a dotted pattern, further proving that the nanostar is a single crystal. This indicates that the formation mechanism of the nanostar involves seeded growth rather than an aggregation of seeded particles or an assembly process of the nanowires.[14] The X-ray diffraction (XRD) pattern (Figure S2) confirms that the carbon-supported Pt nanowires are crystallized in a face-centered-cubic (fcc) structure similar to bulk Pt,[15] which is consistent with the HRTEM investigations.

We believe that the growth of the multiarmed starlike PtNWs on carbon black supports follows a similar process to that for Pt NWs on other supports.[13b] Typically, Pt nuclei are first formed in solution through the reduction of H_2PtCl_6 by HCOOH, and they deposit on the surface of carbon spheres. The freshly formed nuclei act as the sites for further nucleation through the continual absorption and reduction of Pt(IV) ions leading to the formation of particle seeds. For fcc structures, the sequence of surface energies is $\gamma_{\{111\}} < \gamma_{\{100\}}$

© 2011 Wiley-VCH Verlag GmbH & Co. KGaA, Weinheim

Figure 1. A) SEM and B) TEM image of carbon-supported multiarmed starlike Pt nanowire catalyst.
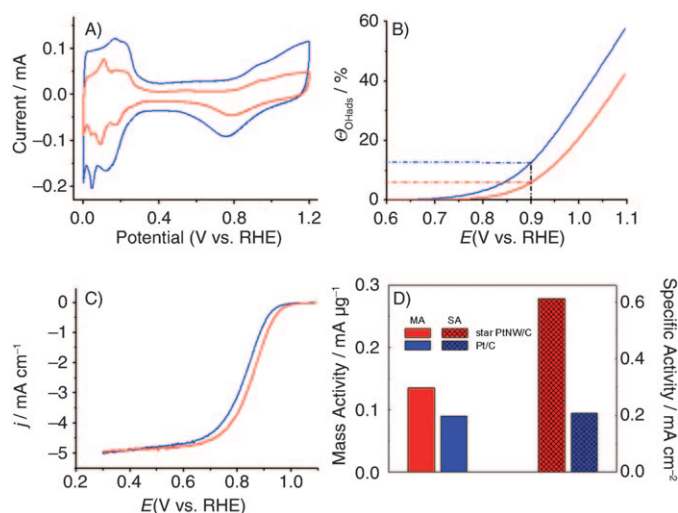

Figure 2. A) CV curves and B) hydroxy surface coverage (Θ_{OH}) for Pt/C (E-TEK, blue curve) and starlike PtNW/C (40 wt% Pt; red curve) catalysts. C) Polarization curves for ORR of Pt/C (E-TEK; blue curve) and starlike PtNW/C catalysts (red curve) in O_2-saturated 0.5 M H_2SO_4 solution at room temperature (1600 rpm, sweep rate 10 mV s^{-1}). D) Mass activity and specific activity at 0.9 V (vs. RHE) for the two catalysts.

$< \gamma_{\{110\}}$, which implies the single-crystal seeds are expected to exist finally as truncated octahedrons enclosed by a mix of {111} and {100} facets in order to maximize the expression of {111} facets and minimize the total surface energy.[16] As the reaction is conducted at room temperature, the reduction rate is very low; therefore, according to the lowest-energy principle, the anisotropic growths along the closed-packed <111> directions are enhanced.[13a] Finally, multiarmed starlike PtNWs are formed based on the truncated octahedron seeds which have several {111} facets. The exact formation mechanism is still under investigation. However, we believe that the key is to reduce the reduction rate of Pt ions, which favors the growth of {111} planes and therefore leads to the formation of 1D nanowires.

We benchmarked the electrochemical properties of starlike PtNW/C against a commercial catalyst made of Pt nanoparticles on carbon support (E-TEK, 30 wt% Pt). Figure 2 A shows the cyclic voltammetry (CV) curves of these two catalysts recorded at room temperature in an Ar-purged H_2SO_4 solution (0.5 M) with a sweep rate of 50 mV s^{-1}. Both CV curves exhibit strong peaks associated with hydrogen adsorption/desorption and Pt oxide formation/reduction. Well-defined multiple hydrogen adsorption and desorption peaks on different Pt low-index surfaces became more definable for the carbon-supported Pt nanowire catalyst. The electrochemical surface areas (ECSA) were calculated by measuring the charge associated with the H_{ads} (Q_H) between 0 and 0.4 V and assuming $Q_{ref} = 0.21$ mC cm^{-2} for the adsorption of a hydrogen monolayer,[17] corresponding to a surface

density of 1.3×10^{15} Pt atoms per cm^2, which is generally accepted for polycrystalline Pt electrodes. The specific ECSA of the starlike PtNW/C was 22.1 m^2 g^{-1} Pt, which is about half (51%) of that of commercial E-TEK Pt/C catalyst (43.3 m^2 g^{-1} Pt). Interestingly, the dimensional change of Pt nanostructures from particle (0D) to wire (1D) also greatly altered the ability to adsorb hydroxy species (OH$_{ad}$, $E > 0.6$ V) (Figure 2 B). Both the onset and peak potentials for the starlike PtNW/C show positive shifts compared with E-TEK carbon-supported Pt nanoparticles on the backward sweep, indicating the fast hydroxy desorption from the Pt nanowires surface.[3c]

Figure 2 C shows typical ORR polarization curves of starlike PtNW/C and Pt/C (E-TEK) catalysts obtained at room temperature in oxygen-saturated 0.5 M H_2SO_4 by using a glassy carbon rotating disk electrode (RDE) at 1600 rpm. The half-wave potentials for the starlike PtNW/C and Pt/C catalysts were 0.848 and 0.813 V, respectively, indicating that the catalytic activity of carbon-supported starlike PtNWs was higher than that of the commercial Pt/C catalyst made of Pt nanoparticles. Mass activity and specific activity are good indicators of the quality of an electrocatalyst. As shown in Figure 2 D, starlike PtNW/C exhibited a mass activity of 0.135 mA µg^{-1} Pt at 0.9 V (vs. RHE), which is 1.5-times greater than that of the Pt/C (E-TEK) catalyst (0.09 mA µg^{-1} Pt). Interestingly, this improvement occurred in spite of about a 50% lower Pt active surface area for starlike PtNW/C catalyst. Taking into account both effects, a specific ORR activity for the starlike Pt NW/C of 0.611 mA cm^{-2} Pt was obtained at 0.9 V, which was nearly three times that for E-TEK Pt/C catalyst (0.207 mA cm^{-2} Pt). This improvement agrees well with those reported for Pt NWs obtained under full cell operating conditions.[9]

The improved activity for the starlike nanowires compared with nanoparticles of Pt could be due to several factors,

including 1) the changes in morphology (1D vs. 0D) because the 1D shape could facilitate the reaction kinetics and improve the O_2 diffusion to Pt surface; 2) fewer surface defects borne by the nanowires which have a closer resemblance to the surface of large single Pt crystals that exhibit even higher ORR specific activities; and 3) the preferential exposure of certain crystal facets of Pt nanowires since the different low-index surfaces have markedly different activities.[9,11,18] In addition, the adsorbed OH_{ad} species on the Pt surface could block the active surface for O_2 adsorption and thus have a negative impact on the ORR. Pt NWs bear comparatively smooth atomic surfaces, which have a small number of low coordination atoms, thus they are more active than surfaces with a high concentration of such sites because of the reduced interaction with OH species. Therefore, the low OH_{ad} coverage on the surface of carbon-supported starlike Pt NW catalyst helps to improve the ORR kinetics, resulting in enhanced activities.[19]

The accelerated durability tests (ADT) of the catalysts were conducted by potential cycling between 0.6 and 1.2 V vs. RHE in O_2-purged H_2SO_4 solution (0.5 M) at room temperature, with scan rate of 50 mV s^{-1}. After 4000 cycles, the starlike PtNW/C catalyst had lost 40% of the Pt initial ECSA (Figure 3 B and D) and showed a degradation of 20 mV in the half-wave potential (Figure S3B), while the degradation of E-TEK Pt/C catalyst was quite severe, with 67.5% loss of the initial Pt ECSA (Figure 3 A and D) and a large decrease of 88 mV in the half-wave potential (Figure S3A). Interestingly, the durability of Pt nanowire catalyst could be further improved by removing the corrosion effect of the carbon support. The ADT tests (Figure 3 C and D) showed that the Pt ECSA of the unsupported Pt NWs decreased about 13% after 4000 cycles, which was 5.2- and 3.1-times better than that of E-TEK Pt/C and carbon-supported PtNW catalysts, respec-

tively. In addition, it showed a quite small negative shift of 9 mV in the half-wave potential (Figure S3C).

The morphology changes of the E-TEK Pt/C, carbon-supported starlike Pt NWs, and unsupported Pt NWs were investigated by TEM before and after ADT cycling (Figure 4 and Figure S4). The Pt nanoparticle size in the E-TEK Pt/C commercial catalyst increased from 2–5 nm to 5–25 nm (by a factor of up to 5). In addition, the density of Pt particles on
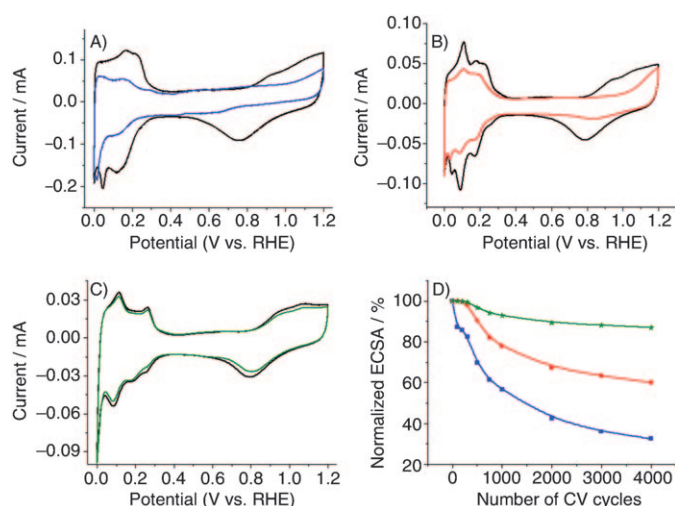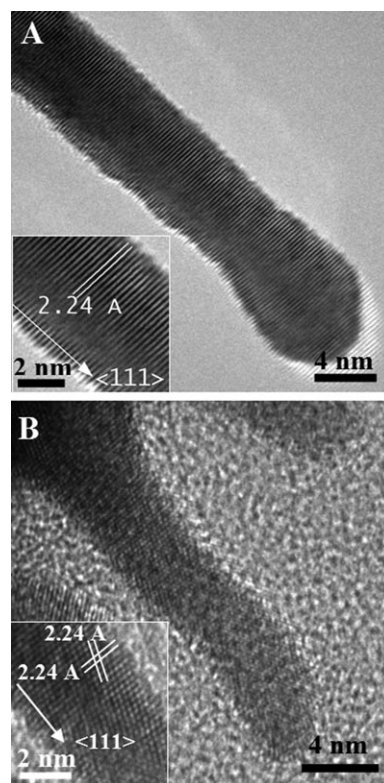

Figure 4. TEM images of unsupported Pt NW A) before, and B) after accelerated CV test. Insets of (A) and (B) show the corresponding HRTEM images, respectively.

carbon became much less, confirming that the major cause for the Pt ECSA loss of Pt/C catalyst was by Pt nanoparticle ripening, the aggregation and falling off of Pt because of corrosion of the carbon support. By contrast, there were no obvious morphological changes for the carbon-supported Pt NW catalyst after ADT cycling. Their star shape and 1D morphology remained the same, with slight aggregation, which might be a result of the corrosion of the carbon support. Meanwhile, the unsupported Pt NWs maintained their 1D morphology and the ⟨111⟩ growth direction after 4000 cycles of ADT test. The diameters of Pt NWs decreased slightly and their surfaces (especially the edges) became rough because of the possible mild dissolution of Pt. This might be the main reason for the small drop in Pt ECSA of unsupported PtNWs. As shown in the schematic illustration of morphology changes that occurred in Pt during accelerated electrochemical cycling (Figure 5), the Ostwald ripening and aggregation of Pt, as well as corrosion of the carbon support in the case of the absence

Figure 3. CV curves for A) Pt/C (E-TEK), B) starlike PtNW/C, and C) unsupported PtNW catalysts before (black curves) and after 4000 cycles (blue, red, and green curves). D) Loss of electrochemical surface area (ECSA) of Pt/C (E-TEK; blue), starlike PtNW/C (red), and unsupported PtNW catalysts (green) as a function of cycling numbers in O_2-purged 0.5 M H_2SO_4 solution at room temperature (0.6–1.2 V vs RHE, sweep rate 50 mV s^{-1}).
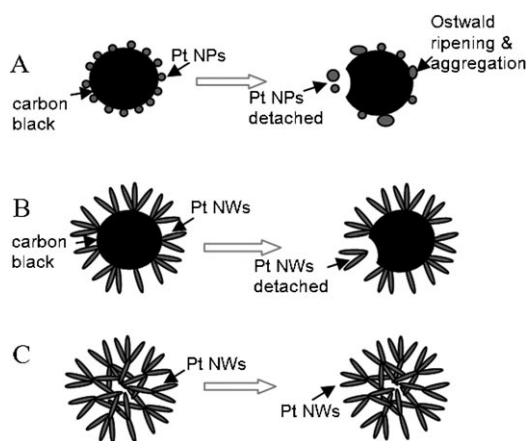
Figure 5. Schematic of morphology changes that occur in Pt during accelerated electrochemical cycling. A) Pt NPs/C (E-TEK), B) Pt NWs/C, and C) unsupported PtNWs.

of carbon, can be significantly mitigated by introducing 1D and the starlike network Pt morphology.[11]

In summary, we have demonstrated a promising electrocatalyst based on starlike Pt nanowires with both good catalytic activity and durability. The novel starlike Pt nanowire structure may also be used in other industrial applications.

Experimental Section

Platinum nanowires were synthesized by the chemical reduction of Pt precursor with formic acid.[13] All the experiments were conducted in aqueous solution, at room temperature and under ambient atmosphere. In a typical synthesis, 0.032 g hexachloroplatinic acid ($H_2PtCl_6 \cdot 6H_2O$, 99.95%, Aldrich) and 1 mL formic acid (HCOOH, 98%, Aldrich) were dissolved in 20 mL H_2O and stored at room temperature for 72 h. The solution turned from golden-orange to grey and then to dark brown. All aqueous solutions were prepared with ultrapure water from a Barnstead Nanopure water system. For the growth of 40 wt% Pt on carbon, a suspension of 7.5 mg carbon black (Vulcan XC72R) in 21 mL reaction solution (14.67 mg $H_2PtCl_6 \cdot 6H_2O$ and 1 mL HCOOH in 20 mL of water) was sonicated for 30 min. After this initial dispersion, the solution is stored at room temperature for 72 h. The product was collected by centrifugation and washed several times with water, and then dried in an oven at 60 °C for further use in characterization and electrochemical measurements.

Scanning electron microscopy (SEM) images were taken on a Hitachi S-4800 microscope, operating at 5 kV. Transmission electron microscopy (TEM) observations were performed with a Philips CM10 microscope at an accelerating voltage of 100 kV. High-resolution TEM (HRTEM) images were obtained with a JEOL 2010F microscope, operating at 200 kV. The Pt loading were confirmed by inductively coupled plasma-optical emission spectroscopy (ICP-OES). Electrochemical properties of the catalysts were measured on an Autolab potentiostat/galvanostat (Model, PGSTAT-30, Ecochemie, Brinkman Instruments) with rotation control (MSR, Pine Instruments) using a three-electrode system that consists of a glassy carbon (GC) rotating disk electrode (RDE), a Pt wire counter electrode, and a Ag/AgCl (3 M NaCl) reference electrode which was separated from the working electrode compartment by a closed electrolyte bridge. For convenience, all potentials in this study are referenced to the reversible hydrogen electrode (RHE). The working electrode was prepared with a procedure similar to the one reported

previously.[20] Typically, the catalyst dispersions were prepared by mixing 5 mg of catalyst in 5 mL aqueous solution containing 1 mL of isopropyl alcohol and 30 μL of 5 wt% Nanfion solution (4:1:0.0017 v/v) followed by 12 min ultrasonication. GC disk electrodes (5 mm diameter, 0.196 cm², Pine Research Instrument) served as the substrate for the support and were polished to a mirror finish. An aliquot of catalyst suspension was pipetted onto the carbon substrate, leading to a Pt loading of about 6 $\mu g_{Pt}\,cm^{-2}$ for all catalysts. The catalyst films were dried under flow N_2 at room temperature.

The working electrode was first cycled between 0 and 1.2 V for 50 times in an Ar-purged H_2SO_4 solution (0.5 M) at room temperature, to produce a clean electrode surface. The scan rate used was 50 mV s^{-1}. Then the cyclic voltammetry (CV) measurements were conducted by cycling the potential between 0 and 1.2 V, with sweep rate of 50 mV s^{-1}. The electrochemical surface areas (ECSA) were calculated by measuring the charge associated with the H_{ads} (Q_H) between 0 and 0.4 V and assuming $Q_{ref} = 0.21$ mC cm^{-2}, corresponding to a surface density of 1.3×10^{15} Pt atoms per cm², which is generally accepted for polycrystalline Pt electrodes. The ECSA of Pt was calculated based on the relation ECSA = $Q_H/(Q_{ref}m)$ where Q_H is the charge for H adsorption (mC cm^{-2}), m is the Pt loading (mg cm^{-2}) in the electrode, and Q_{ref} is the charge required for the monolayer adsorption of hydrogen on a Pt surface (0.21 mC cm^{-2}).[17a] The adsorption of hydroxy species was calculated based on the OH_{ad} peak in the CV curves at the potential larger than 0.6 V. Dividing the hydroxy adsorption area by the overall active surface area resulted in the surface coverage of OH_{ad} species (Θ_{OHad}).[3c] The oxygen reduction reaction (ORR) experiments were performed in oxygen-saturated H_2SO_4 solution (0.5 M) at room temperature. The RDE rotating rate was 1600 rpm and sweep rate was 10 mV s^{-1}. Current densities were normalized in reference to the geometric area of the GC RDE (0.196 cm²). The CV measurements for accelerated durability test (ADT) were conducted by potential cycling between 0.6 and 1.2 V (vs. RHE) for 4000 cycles in O_2-saturated H_2SO_4 solution (0.5 M) at room temperature, with scan rate of 50 mV s^{-1}. Meanwhile, full-scale voltammogram between 0.0 and 1.2 V in N_2-saturated H_2SO_4 solution (0.5 M) were recorded periodically to track the degradation of Pt catalysts.

[1] R. Borup, J. Meyers, B. Pivovar, Y. S. Kim, R. Mukundan, N. Garland, D. Myers, M. Wilson, F. Garzon, D. Wood, P. Zelenay, K. More, K. Stroh, T. Zawodzinski, J. Boncella, J. E. McGrath, M. Inaba, K. Miyatake, M. Hori, K. Ota, Z. Ogumi, S. Miyata, A. Nishikata, Z. Siroma, Y. Uchimoto, K. Yasuda, K. Kimijima, N. Iwashita, *Chem. Rev.* **2007**, *107*, 3904.

[2] Z. M. Peng, H. Yang, *Nano Today* **2009**, *4*, 143.

[3] a) Y. Y. Shao, G. P. Yin, Y. Z. Gao, *J. Power Sources* **2007**, *171*, 558; b) P. J. Ferreira, G. J. la O', Y. Shao-Horn, D. Morgan, R. Makharia, S. Kocha, H. A. Gasteiger, *J. Electrochem. Soc.* **2005**, *152*, A2256; c) Z. M. Peng, H. Yang, *J. Am. Chem. Soc.* **2009**, *131*, 7542.

[4] J. Q. Tian, S. P. Jiang, Z. Liu, L. Li, *Electrochem. Commun.* **2007**, *9*, 1613.

[5] E. Formo, E. Lee, D. Campbell, Y. N. Xia, *Nano Lett.* **2008**, *8*, 668.

[6] Y. S. Kim, S. H. Nam, H. S. Shim, H. J. Ahn, M. Anand, W. B. Kim, *Electrochem. Commun.* **2008**, *10*, 1016.

[7] H. J. Kim, Y. S. Kim, M. H. Seo, S. M. Choi, W. B. Kim, *Electrochem. Commun.* **2009**, *11*, 446.

[8] E. P. Lee, Z. M. Peng, D. M. Cate, H. Yang, C. T. Campbell, Y. N. Xia, *J. Am. Chem. Soc.* **2007**, *129*, 10634.

[9] S. H. Sun, F. Jaouen, J. P. Dodelet, *Adv. Mater.* **2008**, *20*, 3900.

[10] H. J. Zhou, W. P. Zhou, R. R. Adzic, S. S. Wong, *J. Phys. Chem. C* **2009**, *113*, 5460.

[11] Z. W. Chen, M. Waje, W. Z. Li, Y. S. Yan, *Angew. Chem.* **2007**, *119*, 4138; *Angew. Chem. Int. Ed.* **2007**, *46*, 4060.

[12] Y. S. Kim, H. J. Kim, W. B. Kim, *Electrochem. Commun.* **2009**, *11*, 1026.

[13] a) S. H. Sun, D. Q. Yang, D. Villers, G. X. Zhang, E. Sacher, J. P. Dodelet, *Adv. Mater.* **2008**, *20*, 571; b) S. H. Sun, D. Q. Yang, G. X. Zhang, E. Sacher, J. P. Dodelet, *Chem. Mater.* **2007**, *19*, 6376.

[14] M. A. Mahmoud, C. E. Tabor, M. A. El-Sayed, Y. Ding, Z. L. Wang, *J. Am. Chem. Soc.* **2008**, *130*, 4590.

[15] J. Y. Chen, T. Herricks, M. Geissler, Y. N. Xia, *J. Am. Chem. Soc.* **2004**, *126*, 10854.

[16] Y. N. Xia, Y. J. Xiong, B. Lim, S. E. Skrabalak, *Angew. Chem.* **2009**, *121*, 62; *Angew. Chem. Int. Ed.* **2009**, *48*, 60.

[17] a) T. J. Schmidt, H. A. Gasteiger, G. D. Stab, P. M. Urban, D. M. Kolb, R. J. Behm, *J. Electrochem. Soc.* **1998**, *145*, 2354; b) B. Lim, M. J. Jiang, P. H. C. Camargo, E. C. Cho, J. Tao, X. M. Lu, Y. M. Zhu, Y. N. Xia, *Science* **2009**, *324*, 1302.

[18] V. R. Stamenkovic, B. Fowler, B. S. Mun, G. Wang, P. N. Ross, C. A. Lucas, N. M. Markovic, *Science* **2007**, *315*, 493.

[19] a) J. L. Zhang, Y. Mo, M. B. Vukmirovic, R. Klie, K. Sakaki, R. R. Adzic, *J. Phys. Chem. B* **2004**, *108*, 10955; b) J. L. Zhang, M. B. Vukmirovic, Y. Xu, M. Mavrikakis, R. R. Adzic, *Angew. Chem.* **2005**, *117*, 2170; *Angew. Chem. Int. Ed.* **2005**, *44*, 2132.

[20] M. S. Saha, R. Li, M. Cai, X. Sun, *Electrochem. Solid-State Lett.* **2007**, *10*, B130.